Transfer function analysis of welding stage models in Ultrasonic Metal Welding

Elie Abi Raad, Thomas Joyeux-Alcindor, Michael Vorländer

Institute for Hearing Technology and Acoustics, RWTH Aachen University, 52074 Aachen,
E-Mail:ear@akustik.rwth-aachen.de

Introduction

Ultrasonic Metal Welding (USMW) is a friction-welding technique used in numerous industrial applications, such as in welding Lithium-ion battery tabs. USMW can weld metal wires, thin metal sheets, and many other geometries. The metal pieces which are welded are called workpieces. USMW works by applying a static, vertical pressure on the workpieces, and then generating a relative displacement between the workpieces. The vertical pressure and horizontal vibration are applied on the workpieces by the horn, also called sonotrode, which compresses the workpieces and then vibrates horizontally at about 20 kHz. The workpieces are placed on a machine component called "anvil", which acts as a support against which the workpieces are compressed. During welding, relative displacement between the horn, the upper worksheet, lower worksheet and anvil causes friction between them. This ultimately leads to the formation of a weld between the workpieces. Although USMW is widely used, it suffers from unexplained fluctuations in the strength of the welds it produces. Furthermore, the detailed process in which the workpieces form a joint is not clear. This makes it challenging to control the strength of the welds accurately. Multiple theories have been suggested over time, suggesting plastic deformation, chemical interaction, and crystal restructuring of the workpieces as possible mechanisms for joint formation, among others [1][2]. One of the most recent theories on how joints are formed in USMW is from 2020 [1].

In this theory, Balz suggests that the weld formation is chiefly due to one main factor: heat generation due to friction at the interfaces between the horn, the upper worksheet, the lower worksheet and the anvil. The heat generated would lead to a softening of the workpieces, plastic deformation to form the weld, and dynamic recrystallization of the weld to strengthen it. To generate friction, these different elements must move relative to each other. Balz further decomposes the USMW weld formation to six stages, each with distinctive relative displacements of the horn, workpieces and anvil.

The goal of the work presented in this paper is to test the model suggested by Balz by comparing it to measurements. To do this, a mechanical model of the vibrations of the horn, workpieces and anvil during welding is derived from the theory, and a transfer function is derived from it. This transfer function is then compared to the vibrations of the horn and anvil measured during welding.

Theoretical transfer function order

Stage description

In [1], USMW is divided into six stages, each with distinctive relative displacements of the horn, upper workpiece, lower workpiece, and anvil. A short, approximate description of the most important elements of each welding stage will be given here.

The first welding stage happens at the beginning of welding. In this stage, the lower sheet and the anvil are connected, and there is no relative movement between them. The horn and upper worksheet move relative to each other and relative to the lower worksheet and anvil. In this stage, friction at the horn-upper-worksheet and upper-lower worksheets raises the temperature of the worksheets.

In the second welding stage, the lower worksheet and anvil are still connected, and the upper worksheet and horn still move relative to each other and to the lower worksheet and anvil. In this stage, the surface layers of the worksheets are shaved off by the friction and movement between them. The temperature of the worksheets continues to increase.

In the third stage, the horn, upper worksheet, lower worksheet and anvil all move relative to each other. In this stage, the worksheets have softened due to their temperatures, and micro-welds start to form at the points of contact between the workpieces.

In the fourth stage, the worksheets are now joined, and do not move relative to each other. They still move relative to the horn and anvil, and there is therefore friction at the horn-workpiece and the workpiece-anvil interfaces. In this stage, the micro-welds from the previous stage go through a dynamic recrystallization, facilitated by the high temperature and the continued heat into the system by friction. New micro-welds continue to form and to strengthen.

In the fifth stage, the worksheets are still joined, do not move relative to each other, and still move relative to the horn and anvil. In this stage, the joint area is maximised, and the joint reaches its maximum strength.

In the sixth stage, the worksheets, horn and anvil relative movements are similar to the previous stage. However, due to the continued energy into the system, the joint weakens.

General mechanical model

As described in the previous section, the horn, upper worksheet, lower worksheet and anvil move relative to each other during welding, and the amount of relative displacement between them changes during welding. Rather than create a different mechanical model for each stage, a general mechanical model which assumes relative displacement between each of the horn, upper workpiece, lower workpiece and the anvil was chosen. The connections between these different elements are modeled using springs and dampers. Such a model should be able to be fit to any welding stage by changing the value of the spring and damper constants at any interface as required. For example, when the workpieces are joined, then the spring constant between them can be set to

infinity, and the damping constant can be set to 0. The mechanical model can be seen in **Figure 1**.

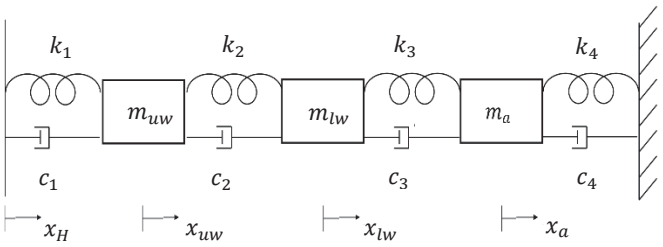

Figure 1: General mechanical model

In this model, the horn is symbolized by the bar at the left-hand side of the plot, where x_h starts from. m_{uw} denotes the mass of the upper workpiece, m_{lw} the mass of the lower workpiece, and m_a the mass of the anvil. The connections at the different interfaces are modelled using springs and dampers: k_1 and c_1 model the connection between the horn and the upper workpiece, k_2 and c_2 that between the two workpieces, and k_3 and c_3 between the lower workpiece and the anvil. k_4 and c_4 model, in a very simplistic way, the transfer of vibrations within the anvil, from the welding site, where the anvil is in contact with the lower workpiece, to the measurement point. The measurement point and the welding site can be seen in **Figure 2**.

Transfer function order

Based on this model, it is possible to derive the equations with Newton's 2nd law (established considering small vibrations around an equilibrium point):

$$m_{uw}\ddot{x}_{uw} = k_1(x_h - x_{uw}) + k_2(x_{lw} - x_{uw}) + c_1(\dot{x}_h - \dot{x}_{uw}) + c_2(\dot{x}_{bw} - \dot{x}_{uw}) \quad (1)$$

$$m_{lw}\ddot{x}_{lw} = k_2(x_{uw} - x_{lw}) + k_3(x_a - x_{lw}) + c_2(\dot{x}_{uw} - \dot{x}_{lw}) + c_3(\dot{x}_a - \dot{x}_{lw}) \quad (2)$$

$$m_a\ddot{x}_a = k_3(x_b - x_a) - k_4x_a + c_3(\dot{x}_{lw} - \dot{x}_a) - c_4x_a \quad (3)$$

From these equations, and setting the Horn as input and the Anvil as output, it is possible to obtain the transfer function G of the system, which is of the form:

$$G = \frac{Anvil}{Horn} = \frac{Output}{Input} = \frac{z_1 s^n + z_2 s^{n-1} + \cdots}{p_1 s^m + p_2 s^{m-1} + \cdots} \quad (4)$$

where, z_i and p_i are the zeros and the poles of the transfer function. n and m are the highest power of s in the numerator and the denominator respectively.

Rather than derive the transfer function by hand, MATLAB was used to find the order of the transfer function. Using the state-space representation and the MATLAB function *ss2tf*, it was found that the transfer function has 6 poles and 3 zeros.

The value of these poles and zeros, the coefficients themselves, still need to be found. This will be done by fitting the transfer function from (4) to the experimental data.

Data acquisition and analysis

To compare the model from the literature to the experiments, the transfer function *G* should be fit to the experimental data.

Experimental data acquisition

The experimental setup was described in details in [3]. The most important information will be repeated here.

For this study, the workpieces were CW-008A copper sheets, welded along their width. The dimensions of the sheets were 125 mm x 45 mm x 0.5 mm (length x width x thickness). The amplitude of vibration of the horn at the welding frequency was 25 µm. The total welding time was about 1.2 s.

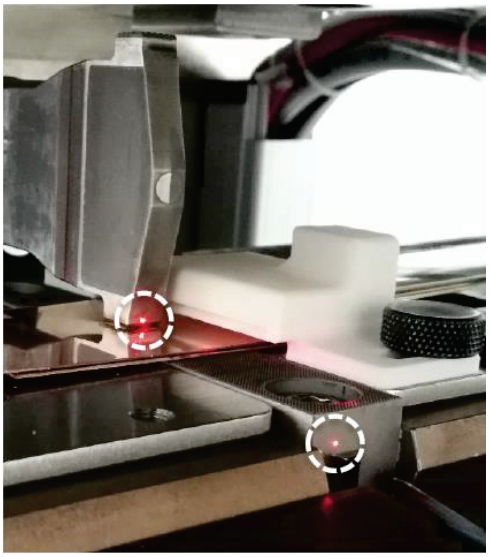

Figure 2: The measurement points of the horn and anvil vibrations are shown in the white circles

Using two laser Doppler vibrometers, the vibrations of the horn and the anvil were measured in the direction of welding during welding. The measurement points are shown in Figure 2, which is repeated from [3]. The velocities measured were denoised with a high-pass filter at 5 kHz and then integrated to get the displacements, which are used in this work. The sampling rate of the system was 250 kHz, and the highest measured frequency was 125 kHz. Results shown in [3] show that the vibrations include a large frequency peak at the welding frequency, 20 kHz, as well as its harmonics up to 120 kHz, and further frequency content as well. The contribution of the welding frequency to the vibrations of the horn and anvil are much higher than the contribution of other frequencies.

For this study, approximately 60 welds spanning all welding stages described by Balz, except for the last stage, overwelding, were made. In [3], these welds are referred to as "Basic+". This last stage involves the destruction of the weld due to a too long welding time. The welding time, pressure, and other welding parameters were chosen based on the experience of the machine operator, and with trial and error.

Of those 60 measurements, 27 were used for this analysis, the other measurements suffering from measurement errors.

Implementation of the evaluation algorithm

The 27 measurements were divided into a training set of 17 samples, and a test set of 10 samples. The training set was used to train the transfer function G; in other words, to find the poles and zeros coefficients. The test set was then used to test how well this transfer function would fit the measurement data. The allocation of measurements into the training set and test set was random.

Furthermore, a sliding window analysis was done. Each measurement was divided into 0.1 s windows with 0.05 s overlap, for a total of 22 windows per measurement. Training the transfer function and testing its fit was done for each one of these 22 windows. In this way, the analysis could capture time changes in the measurement data, and would be able to fit the general mechanical model to different stages well.

For each window of the sliding window analysis, the analysis was done in the following steps.

Training the transfer function

First, the transfer function has to be fitted to the experimental data. In this work, the Output-Error model was chosen, which focuses on the identification of the dynamics of the system and minimises the impact of noise in the measurement [4]:

$$Output = G * Input + E \tag{5}$$

where the Output and the Input are measurements of the anvil and horn vibrations from the training set. This was implemented in MATLAB using the function *oe*. The algorithm is given the input and output of the transfer function as arguments, which are the measured horn and anvil vibrations respectively, and returns the transfer function G. A single transfer function G can also be trained by giving the function an array of inputs and an array of outputs. The error E was not used in this study. The output of this step is a trained transfer function G_{train} .

Testing the fit

Second, the fit of the transfer function has to be tested. To do this, the calculated output $\hat{y}$ had to be created.

$$\hat{y} = G_{train} * Input \tag{6}$$

where $Input$ is one of the horn measurements of the test set. The calculated output $\hat{y}$ is therefore equivalent to the calculated anvil vibrations.

Finally, the difference between the calculated output $\hat{y}$ and the measured output y was calculated and the error was quantified:

$$Error = \frac{||y - \hat{y}||}{||y - \bar{y}||} * 100\% \tag{7}$$

where $\bar{y}$ is the mean measured anvil vibration, y is the measured anvil vibration, and $\hat{y}$ is the calculated anvil vibration. A low error value would therefore be a good fit, and a large value would be a bad fit.

The output of this step is 10 error percentages for each sliding window.

Repeating the analysis

The steps above describe the steps in the implementation for a single allocation of measurements into training set and test set. To avoid any bias from a single allocation, the analysis was repeated for six other distributions of measurements into training set and test set.

The final result is therefore 70 error percentages for each sliding window, 10 for each permutation of the measurements.

Results and discussion

Figure 3 shows the box plots of the error computed for each window, and Figure 4 shows the range of the error for each window.

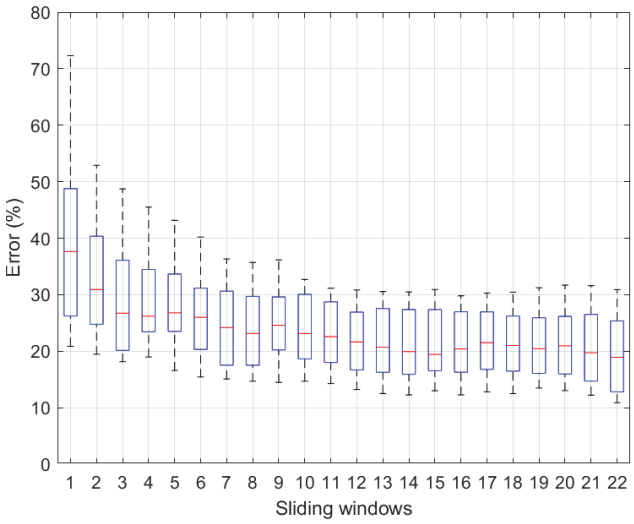

Figure 3: Error box plots for each window

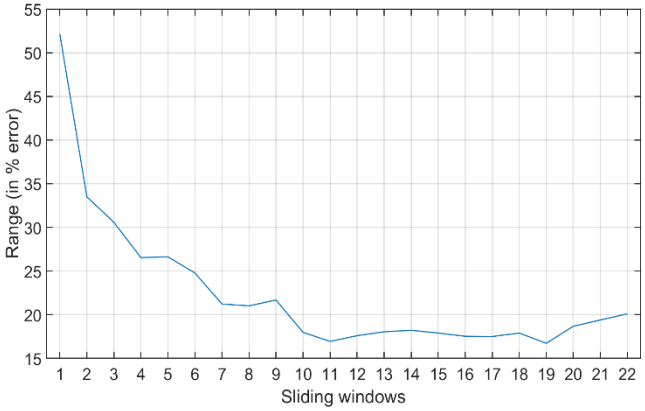

Figure 4: Range of error distribution in each window

In Figure 3, looking at window 1, the median error is 37 %, much higher than in the rest of welding, then decreases until approximately 25 % at window 9, and stays relatively constant around 20 % with small fluctuations until the end of welding.

Looking at the range of the error in Figure 4, the range starts at more than 50% at window 1, decreases until about 22 % at window 9, and then stays below 20 % starting window 10, staying relatively stable around 18 % until window 20. The

range of the error then increases slightly at window 21 and 22, and reaches 20% at window 22.

From colleagues at the Institute of Welding and Joining, RWTH Aachen, where the welds were made, it is believed that around window 9 is when the joint starts to get formed, therefore windows 1 to 9 correspond to the first two stages of USMW, and maybe a part of stage 3. The transfer function derived is therefore a bad fit for the measurement data in stages 1 and 2, and especially in stage 1. This could be due to unaccounted phenomena, such as large amounts of slip between the worksheets at these stages, which would hinder the transfer of vibrations from the horn to the anvil. As the workpieces get better connected, the horn vibrations would get transferred to the anvil measurement point more effectively, leading to a decrease in the median and range of the error until a weld is formed, and the workpieces are perfectly coupled.

Starting window 10, there is a relatively good fit of the transfer function for stages 3, 4 and 5. Furthermore, the start of the weld formation around window 10 is clear and distinguished by the stabilisation of the error and spread.

Looking at the minimum error in Figure 3, the lower error reached is slightly above 10%. From Figure 3, the error is limited to somewhere between 10% and 30%, and does not decrease further. This could be due to a number of factors, for example a limitation of the model and the transfer function found themselves, or due to the presence of some noise in the data. It is possible that further filtering the data, for example band-passing around the welding frequency, could lead to better results. If the limitation comes from the model, it is possible that the modal behaviour of the anvil was not taken adequately into account: in this study, it was modelled as a simple spring-mass-damper system, but could require a more complex model.

Conclusion

In this study, the validity of a theoretical model for USMW was tested by comparison to measurements. The model divides USMW into six stages, and attributes different relative displacements between the horn, upper workpiece, lower workpiece and anvil to each stage. A mechanical model was derived from the theoretical model, and a general transfer function of the model, which would fit all six stages, was derived from that. To compare to experimental measurements, the theoretical transfer function was trained with experimental data, and the fit was tested by comparing to a different set of experimental measurements. This was done by dividing the experimental data into sliding windows, and training and testing the transfer function in each window independently of other windows. Based on the results in this paper, the theoretical model fits the measurement data relatively bad in the first two stages of welding, before a weld is formed between the workpieces, and then relatively well in the later stages of welding, once a weld has been formed. The performance of the theoretical transfer function was limited to errors of 10% to 30 %. Further improvements might be possible by using a more complex mechanical model or by filtering the data to focus on the welding frequency. Once a good transfer function for USMW is found, it might be possible to focus the analysis on the connection between the workpieces, which would directly model the strength of the weld. This would be possible by using simulations to model the transfer of vibrations in the horn from the measurement point through the upper workpiece to the joint, and from the joint through the lower workpiece to the anvil measurement point

Literature

[1] Balz, I.: Prozessanalyse der thermo-mechanischen Vorgänge während der Verbindungsbildung beim Metall-Ultraschallschweißen. Doctoral Dissertation RWTH Aachen University. Aachener Berichte Fügetechnik, Band 3/2020, ISBN 978-3-8440-7537-3, 2020

[2] de Vries, E.: Mechanics and Mechanisms of Ultrasonic Metal Welding. Doctoral dissertation, Ohio State University. ISBN 978-0-4966-9934-6, 2004

[3] Abi Raad, E.; Balz, I.; Reisgen, U.; Vorländer, M.: Derivation of characteristic vibroacoustic parameters in Ultrasonic Sheet Metal Welding. Proc. DAGA 2020 (2020), Hannover, Germany, 1129-1132

[4] Duan, H.; Jia, J. ; Ding, R.: Two-Stage Recursive Least Squares Parameter Estimation Algorithm for Output Error Models. In: Mathematical and Computer Modelling 55 (2012), 1151–1159